HHS Public Access

Author manuscript

J Invest Dermatol. Author manuscript; available in PMC 2015 March 01.

Published in final edited form as:

J Invest Dermatol. 2014 September ; 134(9): 2361–2370. doi:10.1038/jid.2014.174.

Co-localization of cell death with antigen deposition in skin enhances vaccine immunogenicity

Alexandra C.I. Depelsenaire[1], **Stefano C. Meliga**[1], **Celia L. McNeilly**[1], **Frances E. Pearson**[1], **Jacob W. Coffey**[1], **Oscar L. Haigh**[1], **Christopher J. Flaim**[1], **Ian H. Frazer**[2], and **Mark A.F. Kendall**[1,2]

[1]The University of Queensland, Delivery of Drugs and Genes Group, The Australian Institute for Bioengineering and Nanotechnology, St Lucia, QLD 4072, Australia

[2]The University of Queensland, Diamantina Institute for Cancer, Brisbane, QLD 4102, Australia

Abstract

Vaccines delivered to the skin by microneedles – with and without adjuvants – have increased immunogenicity with lower doses than standard vaccine delivery techniques such as intramuscular (i.m.) or intradermal (i.d.) injection. However, the mechanisms behind this skin-mediated ‘adjuvant’ effect are not clear. Here, we show that the dynamic application of a microprojection array (the Nanopatch) to skin generates localized transient stresses invoking cell death around each projection. Nanopatch application caused significantly higher levels (~65-fold) of cell death in murine ear skin than i.d. injection using a hypodermic needle. Measured skin cell death is associated with modeled stresses ~1–10 MPa. Nanopatch-immunized groups also yielded consistently higher anti-IgG endpoint titers (up to 50-fold higher) than i.d. groups after delivery of a split virion influenza vaccine. Importantly, co-localization of cell death with nearby live skin cells and delivered antigen was necessary for immunogenicity enhancement. These results suggest a correlation between cell death caused by the Nanopatch with increased immunogenicity. We propose that the localized cell death serves as a ‘physical immune enhancer’ for the adjacent viable skin cells, which also receive antigen from the projections. This natural immune enhancer effect has the potential to mitigate or replace chemical-based adjuvants in vaccines.

Keywords

vaccine; skin; microneedles; intradermal vaccination; cell death

Correspondence: Mark Kendall, The Australian Institute for Bioengineering and Nanotechnology, The University of Queensland, Corner Cooper and College Rd, St Lucia, QLD 4072, Australia. Phone: +61-7-3346 4203; m.kendall@uq.edu.au.

Conflict of interest

MAFK is a consultant, advisory board member, shareholder of Vaxxas, and inventor on patents licensed to Vaxxas, a company developing the Nanopatch for drug delivery applications. This company has not yet a microprojection-based product, and the microprojection device presented in this study is not directly related to any microprojection devices currently under development at Vaxxas. CJF is employed by Vaxxas through UQ. CJF, ACID and SCM are inventors on a patent application that is licensed to Vaxxas. The other authors state no conflict of interest and have no competing financial interests.

For full method please refer to Supplementary Information online.

Introduction

As conventional vaccine delivery techniques such as intramuscular (i.m.) and subcutaneous (s.c.) injections bypass the skin's immune cells, the skin has increasingly become the target for vaccine delivery (Gutowska-Owsiak and Ogg, 2012; Jiang *et al.*, 2012; Kupper, 2012). Immunizations via skin by intradermal (i.d.) injection have demonstrated similar or improved immunogenicity with commonly reported ~5–10-fold dose-sparing, *i.e*. a significant reduction of antigen required to elicit equivalent immunogenicity compared to other needle-based vaccinations such as i.m. injections against influenza (Auewarakul *et al.*, 2007; Belshe *et al.*, 2004; Hung *et al.*, 2012a; Kenney *et al.*, 2004; Quan *et al.*, 2010; Van Damme *et al.*, 2009), compared to standard i.m. routes. However, difficulties exist in effectively and consistently delivering vaccines into the skin. Therefore, new cutaneous vaccine delivery devices such as microneedles and the Nanopatch (NP) have been developed (Kim *et al.*, 2012a; Koutsonanos *et al.*, 2013;Chen *et al*, 2009), which may also reduce needle-stick injuries, disease transmission of blood-borne diseases (Ekwueme *et al.*, 2002) and could allow for self-administration (Prausnitz *et al.*, 2009). In our previous work, delivery of a conventional influenza vaccine by NP to skin with antigen alone has achieved ~100-fold dose-sparing compared to i.m. delivery (Fernando *et al.*, 2010), while co-delivery of adjuvant generated synergistically-improved antibody and T-cell immune responses (Fernando *et al.*, 2012; Ng *et al.*, 2012).

The NP is a microprojection array with >20,000 cm^{-2} of 100 μm long projections (illustrated in Figure 1a and b) that is applied onto skin at 2.3 ms^{-1} using a spring-loaded applicator, ensuring consistent penetration across the array (Crichton *et al.*, 2010). While i.d. injection deposits vaccine within the vicinity of dermal APCs, previous studies showed that the NP deposits antigen into both viable epidermis (VE) and dermis (Fernando *et al.*, 2010). A contributing factor to improved immunogenicity may be in the mechanical interaction with of the NP with skin. Recently, we have shown that NP projections impacting upon the skin and decelerating upon penetration generate significant stresses within the skin (up to 50 MPa) within a ~20 μm radius around each projection (Meliga *et al.*, 2013). We postulated that such stresses invoke localized cell death and inflammation in the skin, contributing to the improved immune responses generated by NP application by activating APCs to take up antigen.

Following Matzinger's 'danger hypothesis'(Matzinger, 1994), apoptotic and necrotic cells have been reported to act as immunostimulants by releasing damage associated molecular patterns (DAMPs), enhancing cellular and humoral immune responses to antigen (Green *et al.*, 2009; Kinsey *et al.*, 2004; Kono and Rock, 2008; Marichal *et al.*, 2011; Rovere-Querini *et al.*, 2004). Chemical adjuvants have shown to induce cell death and danger signals upon administration which can act as strong endogenous immunostimulatory agents (Marichal *et al.*, 2011; Yang and Shen, 2007; Yang *et al.*, 2004a, b). Disruption of the epidermis by scarification has also been demonstrated as essential for the elicitation of the vaccinia virus-mediated immunity and protection against challenge, whereas i.m. delivery was not protective (Liu *et al.*, 2010).

Here, we hypothesized that localized cell death caused by NP penetrating epidermal and dermal tissue would initiate a cascade of events acting as a ‘natural immune enhancer’, mediated by the release of DAMPS concurrent with antigen delivery. To test this hypothesis, we measured cell death induced *in situ* by a conventional i.d. Mantoux injection and compared it with NP. Systemic immunogenicity was compared using delivered split virion influenza vaccine (Fluvax®). To our knowledge, this is the only quantitative and spatial study published investigating cell death induced by skin immunization on immunogenicity.

Results

Key physical differences in skin surface morphology following Nanopatch application to and intradermal needle injection into skin

We examined the skin surface pre and post NP and 31G needle (hereafter referred to as needle) application *in vivo* and *ex vivo* to gain insights into the skin perforation induced by each device. Using scanning electron microscopy (SEM), we measured the contact area between each device with skin surface (Figure 1b, 1d-f). Untreated murine ear skin revealed an intact surface (Figure 1c), while NP application produced microchannels, consistent with the spacing of projections on an NP (Figure 1d), similar to previous observations (Crichton *et al.*, 2010; Haq *et al.*, 2009; Milewski *et al.*, 2010). I.d. insertion using a needle resulted in a single perforation at the needle insertion site (Figure 1e and 1f, arrows), while saline delivery resulted in the formation of a bleb (Figure 1g). The calculated contact surface area between skin and NP projections was 17.7 ± 2.3 mm^2 (n=18), while 1.6 ± 0.1 mm^2 (n=10) of the needle tip made contact with skin. Coating of Coomassie blue dye allowed visualization of microchannels inflicted by NP, and confirmed coated payload delivery discretely into each microchannel, where it had dissolved off the projection upon application due to rehydration within the skin (Figure 1h, left). Coomassie blue dye injected i.d. allowed further visualization of the bleb (Figure 1h, right). The affected skin area following NP application (Figure 1h inset and 1i) measured 1.9 ± 0.1 mm^2, significantly less than the delivery area of a needle: 27 ± 11 mm^2 (p<0.001; Figure 1h and 1i). Combined, these data demonstrate significant perforation of skin and discrete microchannel delivery following NP application in contrast to a single i.d. delivery to a much larger area in the form of a bleb when using a needle to inject i.d.

Nanopatch™ application to skin induces significantly higher and localized cell death, compared to standard needle-based i.d. injection

We next examined and quantified cellular damage caused within the skin by NP and i.d. needle over a 16 mm^2 area (an area equivalent to a single NP) by Confocal and Multiphoton Microscopy (CLSM/ MPM). (Figure 1e–g). We freshly excised skin immediately after NP application or i.d. injection of PBS, and stained with an acridine orange/ ethidium bromide (AOEB) cocktail to distinguish live and dead cells, respectively (Figure 2a and 2b) (Raju *et al.*, 2006). Untreated skin contained 3.5%±1.9% (n=18) damaged cells (Figure 2c). After NP application, 16.5%±4.1% (n=18) of epithelial cells were dead (Figure 2c), significantly more than untreated skin (p<0.0001). Following NP application, dead cells were restricted to a zone of up to 5 cell radii, or 26±13 µm (n=81 projections), around each microchannel perforation with interspersed viable cells. High levels of cell death were observed where the edges of the NP and skin interacted, consistent with the theoretically-modelled stress peaks at the array boundaries (Meliga *et al.*, 2013).

The cellular damage caused by i.d. injection of saline was restricted to the individual needle perforation site (Figure 2a and 2b), inducing 3.7% ± 1.8% (n=18) of dead cells, similar to untreated skin control. Cell death within the i.d. bleb was statistically similar in comparison to untreated control groups (2.5% ± 1.1%; p=0.16, n=5). Normalized against untreated control groups, i.d. injection generated 65-fold fewer dead cells than NP application. The area of dead cells within the bleb area skin represented <0.5% of the total bleb area (~0.07 mm^2). Cross-sectional MPM images demonstrated that damaged tissue in NP-treated samples was mostly confined to the VE, while delivery by needle resulted in cell death spread throughout the VE and dermal layers (Figure 2b). The observed dead cells exhibited predominantly necrotic characteristics, which was further supported by the absence of apoptotic cell morphology (*i.e.* fragmented nuclei or crescent-shaped nuclei (Cobb *et al.*, 1996; Hotchkiss *et al.*, 2009). Further morphological, biochemical and protein-based analyses are required to further distinguish the cell death types. Collectively, these data highlight key differences between the location of live/ dead cells and a delivered payload (*e.g.* vaccine).

Delivery of vaccine to skin by Nanopatch induces a significantly greater antibody response than standard intradermal delivery by needle

With the local skin cell death and delivered payload profiles quantified, we next compared the resultant systemic immune responses elicited by NP and i.d. immunization routes (Figure 3) by comparing antibody responses to Fluvax® spanning 3 logs of delivered antigen doses. Endpoint titers from all doses of Fluvax® tested were higher after NP delivery than those elicited by i.d. delivery with statistical significant differences detected with delivered doses between 1–100 ng (Figure 3). In addition, all mice given a dose of 5 ng to 100 ng by NP seroconverted, and mean titers (10–100 ng) did not differ statistically from those of the i.m. control group (Supplementary Figure S1). In contrast, ≥50 ng of Fluvax® delivered i.d. was required to achieve seroconversion in all mice. (p<0.001; Figure 3 and Supplementary Figure S1). Together, these data demonstrated robust antibody titers in mice immunized with NP-delivered Fluvax®, compared to i.d. injected mice, illustrating a ≥10-fold dose-sparing effect.

Co-localized Nanopatch-mediated skin damage, adjacent live cells and vaccine enhances systemic immunogenicity

From our immunogenicity results, we hypothesized that co-localization of antigen with Nanopatch-mediated skin damage adjacent to live cells was a key contributing factor to enhanced systemic immunogenicity. To test this hypothesis, we imaged co-localization of Nanopatch-mediated skin damage *in vivo*, adjacent to live cells with fluorescently-labeled (Dylight® 755) Fluvax® (FV) antigen. Labeled antigen was administered by either NP or i.d. injection and animals were imaged within 5 min post immunization *in vivo* to limit diffusion of the antigen (rainbow-colored; Figure 4). In NP-treated samples, 100% of dead cells (orange) co-localized completely with fluorescently-labeled antigen by NP delivery, covering an area of 16 mm^2. Based on the cell death profiles, Coomassie Blue data and diffusion profiles (Raphael *et al.*, 2013), co-localization of antigen with dead cells was much less pronounced with i.d. delivered antigen (<0.5%) as indicated by the arrows (Figure 4), suggesting lower co-localization of antigen with dead cells (and therefore less DAMPs). These observations of co-localizing cell death with antigen are consistent with our previous results (Figure 1h and 2).

While we identified that more antigen overlapped (co-localized) with dead cells following NP than i.d. immunizations (Figure 4), it was not clear whether co-localization of antigen with dead cells interspersed with live cells was essential for enhanced antibody production. To explore this, we compared antibody responses (10 ng Fluvax®) between mice using NP, i.d. or with a combination, as depicted in Figure 5a). In accordance with Figure 3, Fluvax® delivered by NP elicited higher antibody responses than i.d. (Figure 5b; $p<0.05$). Application of an NP or an FP (inducing ~3.8% of cell death; Supplementary Figure S2) immediately prior to i.d. delivered Fluvax® did not enhance the resultant immunogenicity of i.d. generated beyond that obtained with i.d. delivery of Fluvax® alone. We interpret this result as: co-localization of tissue damage caused by NP with antigen is important for enhanced immunogenicity. Similar results were obtained when repeated with a 1 ng Fluvax® dose (Supplementary Figure S3). Taken together, with the results in Figure 4, these data demonstrated that co-localization of antigen with NP-induced cellular damage correlated with enhanced immunogenicity of NP-delivered Fluvax®.

Since i.d. injections resulted in a ~14-fold larger antigen delivery area than NPs (Figure 1h and 1i), we then evaluated whether altering i.d. injection volumes and hence concentrations/ area while maintaining the same delivered dose (5 ng), may affect the systemic immunogenicity. Administering 5 ng Fluvax® by i.d. in different volumes (5–50 μl), with the highest concentration tested injected i.d. was similar to the concentration of a dry-coated NP (2.5 ng/ μl). This difference in antigen concentration did not affect immunogenicity (data not shown). Antigen-specific endpoint titers did not significantly differ between any i.d. groups ($p>0.05$; Figure 5c). These results indicated that vaccine concentration (ranging 1–0.1 ng/ μl) did not affect the immunogenicity in i.d. immunizations.

To further examine the correlation between cell death and enhanced immunogenicity, we extended NP conditions to provide lower and higher levels of cell death – by changing the number of projections cm^{-2} while maintaining all other parameters constant including the delivered dose (assessed as previously described, Fernando *et al.*, 2012). Cell death was quantified while influenza-specific IgG was measured after delivering 1 ng Fluvax® by NPs of varying projectionscm^{-2} (ranging from 10,000, 21,000 to 3x 21,000) or by i.d. injection. As expected, cell death increased with increasing numbers of projections cm^{-2} almost linearly (R^2=0.89), resulting in 2.3% ± 1.0% (untreated), 3.1% ± 1.0% (i.d.), 8.1% ± 1.1% (10,000), 16.2% ± 1.7% (21,000) or 45.4% ± 4.0% (3x 21,000 projections cm^{-2}) (Figure 5d–f left). This indicated that the localized cell death per projection was consistent. Figure 5f (right) illustrated that increased cell death correlated with increased immune responses, with one notable exception: extending to the highest level of cell death (induced by 3x 21,000 NP projections cm^{-2}) led to a significant decrease (p=0.0074) in antibody response compared to a single NP with 21,000 projections.

Discussion

Several different mechanical methods exist for delivering vaccines into skin such as either needle-based or needle-free approaches (Kim *et al.*, 2012a; Kim *et al.*, 2012b; Kis *et al.*, 2012). The delivery of conventional protein and live viral vaccines using these devices has resulted in comparable systemic immune responses to those achieved by standard i.d. injection (Carey *et al.*, 2011; Hung *et al.*, 2012b; Kim *et al.*, 2012b). Here, we compared the application two transcutaneous immunization devices into skin. We used either NP, standard needle-based i.d. injection, or combinations of both methods, and quantified the resultant cell death (including magnitude and location within skin) as well as the systemic immunogenicity generated by influenza vaccination. Overall, we found that NP immunization consistently produced higher antibody titers than standard needle-based i.d. immunizations, which correlated with higher cell death levels after NP than i.d. injections. We propose that the observed improved immunogenicity in NP groups is linked to antigen co-localizing within defined areas of live cells adjacent to dead cells within epidermal and dermal tissue (Figure 4); this was not seen with i.d. injection.

The concept that cell death or co-delivering dead cells with antigens enhances immunogenicity is well known (Green *et al.*, 2009; Kinsey *et al.*, 2004; Kojima *et al.*, 2007; Kono and Rock, 2008; Rovere-Querini *et al.*, 2004). Similarly, others found that DNA released by dead cells mediates adjuvanticity of aluminium salts (Marichal *et al.*, 2011). Increasing the number of NP projections penetrating the skin and thus increasing localized cell death led to improved immunogenicity, until a plateau was reached, after which the immunogenicity decreased (Figure 5d–f). This type of curve is homologous to dose ranging vs. immunogenicity that shows similarity with titration curves of chemical adjuvant doses (unpublished observations and Ng *et al.*, 2012). A key difference however is that in our study, we propose the immune enhancing effect is generated by the mechanical stimulus of the NP being applied to the skin, generating localized cell death.

Recently, laser-based adjuvantation gained interest as potential immune enhancer (Chen *et al.*, 2010) that worked synergistically with other chemical adjuvants (Chen *et al.*, 2012). A ‘physical adjuvantation effect’ of the laser was stipulated (Chen *et al.*, 2013). In agreement with our study, colocalization of the laser beam and immunization site was essential for enhanced immunogenicity. We speculate that laser-induced cell damage/ death (and associated DAMP release) colocalized with antigen and thus enhanced immunogenicity similar to the synergistic effect with chemical adjuvants. A key difference in our study in comparison to others was however that the immune enhancer effect was generated by the NP application itself, generating localized cell death. I.d. injection generated significantly lower cell death, therefore DAMPS may have co-localized less with antigen and live cells; this is summarized schematically in Figure 6a. With live cells immediately adjacent to dead cells sensing danger signals and chemokine/ cytokine gradients required for their activation, and with interspersed vaccine, these live cells may be considered as the target cells to which antigen should be delivered to for enhanced immune responses. Therefore, we believe that a certain threshold of cell death is beneficial to augment immunogenicity to an antigen, beyond which cell death becomes detrimental. This would further support the hypothesis of the NP-induced cell death acting as ‘natural immune enhancer’ contributing to enhanced immunogenicity, compared to standard i.d. injection.

The markedly lower cell death after i.d. injection was localized to a single needle insertion site. Previous investigations of skin cell death induced by mechanical vaccine delivery devices such as tattooing devices were reported to induce necrosis and inflammatory cell infiltration (Gopee *et al.*, 2005) with increased cellular and humoral immune responses (Pokorná *et al.*, 2008). Further, ballistic delivery of micro-particles found >90% dead cells in the center of the target site with only the skin target periphery containing both live/ dead cells (Raju *et al.*, 2006). Our experimental findings contrast Raju *et al.*’s findings most likely due to the inherently different device and application velocities (2.3 ms^{-1} vs. >100 ms^{-1}). However, our experimental findings are consistent with our modeled stress-contours induced by NP application to skin (Figure 6b), where cell death and highest simulated stress levels (red) overlap at the site of projections penetrating the skin (applying previously published mechanical models; Meliga *et al.*, 2013). Qualitative comparison of the spatial distributions of theoretical stress with measured cell death suggests that cells die in regions where Von-Mises stresses of at least 1–10 MPa are generated, subject to modelling assumptions (Meliga *et al.*, 2013). This is the only time that skin cell death has been linked to stress distribution and magnitude to our knowledge.

The type of induced cell death is likely to be important as necrotic cells are generally more immunogenic than apoptotic cells (Rock and Kono, 2008). We speculate that the visualized dead cells are predominantly of necrotic origin, which is in agreement with Gopee *et al.*, who observed necrotic cell death following tattooing in skin (Gopee *et al.*, 2005). Necrotic cell death is further supported by the dynamic application of the NP generating instantaneous stresses and stress-induced trauma in Figure 6b (detailed analysis on the stresses in Meliga *et al.*, 2013) and the absence of apoptotic cell characteristics (Cobb *et al.*, 1996; Hotchkiss *et al.*, 2009) post NP/ i.d. application. Further studies are required to distinguish the type of cell death.

In conclusion, our work herein proposes that physically induced cell death by an immunization device co-delivering antigen into the skin can significantly improve the immunogenicity of vaccines by physical immune enhancement. This is a significant departure from the current adjuvant paradigm, generated by chemical or biological reagents added to antigens to enhance immune responses that are delivered into the body.

Materials and Methods

Materials

Seasonal human trivalent influenza vaccine (Fluvax® 2010) was manufactured by CSL Limited (Parkville, VIC, Australia), containing 15 μg haemagglutinin per strain per dose of purified, inactivated, detergent-disrupted split virion influenza virus with antigen of the following strains: A/California/7/2009, A/Wisconsin/15/2009 and B/Brisbane/60/2008).

Mice

Female 6–8 week old BALB/c or C57BL/6J mice were obtained from the Australian Research Council (Perth, WA). Anesthesia was performed by intraperitoneal (i.p.) injection of ketamine and xylazil anesthetic (50 mg/ kg and 10 mg/ kg; Troy laboratories Pty., Ltd., Smithfield, Australia) prior to immunizations. Mice were euthanized by cervical dislocation either immediately or at indicated time points after treatment. All animal experiments were conducted according to the University of Queensland Anatomical Biosciences Ethics Committee regulations.

Immunizations

The NP was fabricated from silicon using a deep reactive ion etching process at the University of Queensland (Jenkins *et al.*, 2012). Coating solutions for NP were prepared as previously described (Chen *et al.*, 2011; Chen *et al.*, 2009), with coated projections examined by SEM and delivery efficiency verified (Fernando *et al.*, 2012). The NP was applied using a spring-loaded applicator (Crichton *et al.*, 2010) at ~2.3 ± 0.2 ms^{-1} and applied for 2 min. NP and i.d. injections (31G, 20 µl) were administered into the ventral site of murine ears while i.m. injections were given into both hind legs into the caudal thigh muscle (29G; 33 µl).

Viability staining of tissue

To discriminate between live and dead cells, a mixture of metachromatic acridine orange (AO) and ethidium bromide (EB; both Fluka, Steinheim, Germany) in PBS was used (Franklin and Locker, 1981; Raju *et al.*, 2006). AO and EB are routinely used to discriminate between live and dead cells in cell suspensions and tissue by intercalating with DNA and RNA (Baskic *et al.*, 2006; Darzynkiewicz *et al.*, 1992). Tissues were split at the dermis-cartilage-dermis junction with cartilage carefully removed prior to staining in AO (0.03 µg/ ml) and EB (0.1 µg/ ml). Positive controls for cell death were pre-treated with ice-cold methanol prior to staining (Skala *et al.*, 2005). Confocal and Multiphoton Microscopy was used for visualization purposes.

Supplementary Material

Refer to Web version on PubMed Central for supplementary material.

Acknowledgments

The authors would like to thank Dr. Michael Crichton for assistance with cryo-SEM performed at CMM, staff from AMMRF/CMM/ANFF for assistance with the equipment, and Dr. Germain Fernando for reading the manuscript. This research was funded by the ARC Discovery Scheme (MAFK and IHF, Grants ID# DP130100996) and the NHMRC of Australia (MAFK and MSR, Grants ID# APP11049906). IHF was funded in part by NIH grant 5U01-CA141583. ACID is a recipient of UQRS/UQIRTA.

Abbreviations used

AO	acridine orange
EB	ethidium bromide

AOEB	acridine orange and ethidium bromide
SC	*stratum corneum*
VE	viable epidermis
i.d	intradermal
i.m	intramuscular
APCs	antigen presenting cells
NP	Nanopatch
FP	flat patch
DAMPs	damage associated molecular patterns
CLSM	confocal laser scanning microscope
MPM	multiphoton microscopy
MIP	maximum intensity projection

References

Auewarakul P, Kositanont U, Sornsathapornkul P, Tothong P, Kanyok R, Thongcharoen P. Antibody responses after dose-sparing intradermal influenza vaccination. Vaccine. 2007; 25:659–63. [PubMed: 17011678]

Baskic D, Popovic S, Ristic P, Arsenijevic NN. Analysis of cycloheximide-induced apoptosis in human leukocytes: Fluorescence microscopy using annexin V/propidium iodide versus acridin orange/ethidium bromide. Cell Biol Int. 2006; 30:924–32. [PubMed: 16895761]

Belshe RB, Newman FK, Cannon J, Duane C, Treanor J, Van Hoecke C, Howe BJ, Dubin G. Serum Antibody Responses after Intradermal Vaccination against Influenza. N Engl J Med. 2004; 351:2286–94. [PubMed: 15525713]

Carey JB, Pearson FE, Vrdoljak A, McGrath MG, Crean AM, Walsh PT, Doody T, O'Mahony C, Hill AVS, Moore AC. Microneedle Array Design Determines the Induction of Protective Memory CD8+ T Cell Responses Induced by a Recombinant Live Malaria Vaccine in Mice. PLoS ONE. 2011; 6:e22442. [PubMed: 21799855]

Chen X, Fernando GJP, Crichton ML, Flaim C, Yukiko SR, Fairmaid EJ, Corbett HJ, Primiero CA, Ansaldo AB, Frazer IH, Brown LE, Kendall MAF. Improving the reach of vaccines to low-resource regions, with a needle-free vaccine delivery device and long-term thermostabilization. J Control Release. 2011; 152:349–55. [PubMed: 21371510]

Chen X, Kim P, Farinelli B, Doukas A, Yun S-H, Gelfand JA, Anderson RR, Wu MX. A Novel Laser Vaccine Adjuvant Increases the Motility of Antigen Presenting Cells. PLoS ONE. 2010; 5:e13776. [PubMed: 21048884]

Chen X, Pravetoni M, Bhayana B, Pentel PR, Wu MX. High immunogenicity of nicotine vaccines obtained by intradermal delivery with safe adjuvants. Vaccine. 2012; 31:159–64. [PubMed: 23123021]

Chen X, Prow TW, Crichton ML, Jenkins DWK, Roberts MS, Frazer IH, Fernando GJP, Kendall MAF. Dry-coated microprojection array patches for targeted delivery of immunotherapeutics to the skin. J Control Release. 2009; 139:212–20. [PubMed: 19577597]

Chen X, Wang J, Shah D, Wu MX. An update on the use of laser technology in skin vaccination. Expert Rev Vaccines. 2013; 12:1313–23. [PubMed: 24127871]

Cobb JP, Hotchkiss RS, Karl IE, Buchman TG. Mechanisms of cell injury and death. Br J Anaesth. 1996; 77:3–10. [PubMed: 8703628]

Crichton ML, Ansaldo A, Chen X, Prow TW, Fernando GJP, Kendall MAF. The effect of strain rate on the precision of penetration of short densely-packed microprojection array patches coated with vaccine. Biomaterials. 2010; 31:4562–72. [PubMed: 20226519]

Darzynkiewicz Z, Bruno S, Bino GD, Gorczyca W, Hotz MA, Lassota P, Traganos F. Features of apoptotic cells measured by flow cytometry. Cytometry. 1992; 13:795–808. [PubMed: 1333943]

Ekwueme DU, Weniger BG, Chen RT. Model-based estimates of risks of disease transmission and economic costs of seven injection devices in sub-Saharan Africa. Bull World Health Organ. 2002; 80:859–70. [PubMed: 12481207]

Fernando GJP, Chen X, Primiero CA, Yukiko SR, Fairmaid EJ, Corbett HJ, Frazer IH, Brown LE, Kendall MAF. Nanopatch targeted delivery of both antigen and adjuvant to skin synergistically drives enhanced antibody responses. J Control Release. 2012; 159:215–21. [PubMed: 22306334]

Fernando GJP, Chen X, Prow TW, Crichton ML, Fairmaid EJ, Roberts MS, Frazer IH, Brown LE, Kendall MAF. Potent Immunity to Low Doses of Influenza Vaccine by Probabilistic Guided Micro-Targeted Skin Delivery in a Mouse Model. PLoS ONE. 2010; 5:e10266. [PubMed: 20422002]

Franklin W, Locker J. Ethidium bromide: a nucleic acid stain for tissue section. J Histochem Cytochem. 1981; 29:572–6. [PubMed: 6166660]

Gopee NV, Cui Y, Olson G, Arbritton WAR, Miller BJ, Couch LH, Wamer WG, Howard PC. Response of mouse skin to tattooing : Use of SKH-1 mice as a surrogate model for human tattooing. Toxicol Appl Pharmacol. 2005; 209:145–58. [PubMed: 15913690]

Green DR, Ferguson T, Zitvogel L, Kroemer G. Immunogenic and tolerogenic cell death. Nat Rev Immunol. 2009; 9:353–63. [PubMed: 19365408]

Gutowska-Owsiak D, Ogg GS. The epidermis as an adjuvant. J Invest Dermatol. 2012; 132:940–8. [PubMed: 22217742]

Haq M, Smith E, John D, Kalavala M, Edwards C, Anstey A, Morrissey A, Birchall J. Clinical administration of microneedles: skin puncture, pain and sensation. Biomedical Microdevices. 2009; 11:35–47. [PubMed: 18663579]

Hotchkiss RS, Strasser A, McDunn JE, Swanson PE. Cell Death. N Engl J Med. 2009; 361:1570–83. [PubMed: 19828534]

Hung IFN, Levin Y, To KKW. Quantitative and qualitative analysis of antibody response after dose sparing intradermal 2009 H1N1 vaccination. Vaccine. 2012a; 30:2707–8. [PubMed: 22210225]

Hung IFN, Levin Y, To KKW, Chan K-H, Zhang AJ, Li P, Li C, Xu T, Wong T-Y, Yuen K-Y. Dose sparing intradermal trivalent influenza (2010/2011) vaccination overcomes reduced immunogenicity of the 2009 H1N1 strain. Vaccine. 2012b; 30:6427–35. [PubMed: 22910287]

Jenkins D, Corrie S, Flaim C, Kendall M. High density and high aspect ratio solid micro-nanoprojection arrays for targeted skin vaccine delivery and specific antibody extraction. Rsc Advances. 2012; 2:3490–5.

Jiang X, Clark RA, Liu L, Wagers AJ, Fuhlbrigge RC, Kupper TS. Skin infection generates non-migratory memory CD8 + T RM cells providing global skin immunity. Nature. 2012; 483:227–31. [PubMed: 22388819]

Kenney RT, Frech SA, Muenz LR, Villar CP, Glenn GM. Dose Sparing with Intradermal Injection of Influenza Vaccine. N Engl J Med. 2004; 351:2295–301. [PubMed: 15525714]

Kim Y-C, Park J-H, Prausnitz MR. Microneedles for drug and vaccine delivery. Advanced Drug Delivery Reviews. 2012a; 64:1547–68. [PubMed: 22575858]

Kim YC, Jarrahian C, Zehrung D, Mitragotri S, Prausnitz MR. Delivery systems for intradermal vaccination. Curr Top Microbiol Immunol. 2012b; 351:77–112. [PubMed: 21472533]

Kinsey BM, Marcelli M, Song L, Bhogal BS, Ittmann M, Orson FM. Enhancement of both cellular and humoral responses to genetic immunization by co-administration of an antigen-expressing plasmid and a plasmid encoding the pro-apoptotic protein Bax. J Gene Med. 2004; 6:445–54. [PubMed: 15079819]

Kis EE, Winter G, Myschik J. Devices for intradermal vaccination. Vaccine. 2012; 30:523–38. [PubMed: 22100637]

Kojima Y, Jounai N, Takeshita F, Nakazawa M, Okuda K, Watabe S, Xin K-Q, Okuda K. The degree of apoptosis as an immunostimulant for a DNA vaccine against HIV-1 infection. Vaccine. 2007; 25:438–45. [PubMed: 17079059]

Kono H, Rock KL. How dying cells alert the immune system to danger. Nat Rev Immunol. 2008; 8:279–89. [PubMed: 18340345]

Koutsonanos DG, Compans RW, Skountzou I. Targeting the skin for microneedle delivery of influenza vaccine. Adv Exp Med Biol. 2013; 785:121–32. [PubMed: 23456844]

Kupper TS. Old and new: Recent innovations in vaccine biology and skin T cells. J Invest Dermatol. 2012; 132:829–34. [PubMed: 22237702]

Liu L, Zhong Q, Tian T, Dubin K, Athale SK, Kupper TS. Epidermal injury and infection during poxvirus immunization is crucial for the generation of highly protective T cell-mediated immunity. Nat Med. 2010; 16:224–7. [PubMed: 20081864]

Marichal T, Ohata K, Bedoret D, Mesnil C, Sabatel C, Kobiyama K, Lekeux P, Coban C, Akira S, Ishii KJ, Bureau F, Desmet CJ. DNA released from dying host cells mediates aluminum adjuvant activity. Nat Med. 2011; 17:996–1002. [PubMed: 21765404]

Matzinger P. Tolerance, Danger, and the Extended Family. Annu Rev Immunol. 1994; 12:991–1045. [PubMed: 8011301]

Meliga SC, Flaim C, Veidt M, Kendall MA. The mechanical stress caused by microprojection arrays penetrating the skin for vaccine delivery. Journal of Multi-disciplinary Engineering. 2013; 10:173–84.

Milewski M, Brogden NK, Stinchcomb AL. Current aspects of formulation efforts and pore lifetime related to microneedle treatment of skin. Expert Opin Drug Deliv. 2010; 7:617–29. [PubMed: 20205604]

Ng H-I, Fernando GJP, Kendall MAF. Induction of potent CD8+ T cell responses through the delivery of subunit protein vaccines to skin antigen-presenting cells using densely packed microprojection arrays. J Control Release. 2012; 162:477–84. [PubMed: 22841796]

Pokorná D, Rubio I, Müller M. DNA-vaccination via tattooing induces stronger humoral and cellular immune responses than intramuscular delivery supported by molecular adjuvants. Genetic Vaccines and Therapy. 2008; 6:4. [PubMed: 18257910]

Prausnitz MR, Mikszta JA, Cormier M, Andrianov AK. Microneedle-based vaccines. Curr Top Microbiol Immunol. 2009; 333:369–93. [PubMed: 19768415]

Quan F-S, Kim Y-C, Compans RW, Prausnitz MR, Kang S-M. Dose sparing enabled by skin immunization with influenza virus-like particle vaccine using microneedles. J Control Release. 2010; 147:326–32. [PubMed: 20692307]

Raju PA, McSloy N, Truong NK, Kendall MAF. Assessment of epidermal cell viability by near infrared multi-photon microscopy following ballistic delivery of gold micro-particles. Vaccine. 2006; 24:4644–7. [PubMed: 16168530]

Raphael AP, Meliga SC, Chen X, Fernando GJP, Flaim C, Kendall MAF. Depth-resolved characterization of diffusion properties within and across minimally-perturbed skin layers. J Control Release. 2013; 166:87–94. [PubMed: 23266447]

Rock KL, Kono H. The Inflammatory Response to Cell Death. Annual Review of Pathology: Mechanisms of Disease. 2008; 3:99–126.

Rovere-Querini P, Capobianco A, Scaffidi P, Valentinis B, Catalanotti F, Giazzon M, Dumitriu IE, Müller S, Iannacone M, Traversari C, Bianchi ME, Manfredi AA. HMGB1 is an endogenous immune adjuvant released by necrotic cells. European Molecular Biology Organization. 2004; 5:825–30.

Skala MC, Squirrell JM, Vrotsos KM, Eickhoff JC, Gendron-Fitzpatrick A, Eliceiri KW, Ramanujam N. Multiphoton Microscopy of Endogenous Fluorescence Differentiates Normal, Precancerous, and Cancerous Squamous Epithelial Tissues. Cancer Res. 2005; 65:1180–6. [PubMed: 15735001]

Van Damme P, Oosterhuis-Kafeja F, Van der Wielen M, Almagor Y, Sharon O, Levin Y. Safety and efficacy of a novel microneedle device for dose sparing intradermal influenza vaccination in healthy adults. Vaccine. 2009; 27:454–9. [PubMed: 19022318]

Yang Y-W, Shen S-S. Enhanced antigen delivery via cell death induced by the vaccine adjuvants. Vaccine. 2007; 25:7763–72. [PubMed: 17928111]

Yang Y-W, Wu C-A, Morrow WJW. The apoptotic and necrotic effects of tomatine adjuvant. Vaccine. 2004a; 22:2316–27. [PubMed: 15149791]

Yang Y-W, Wu C-A, Morrow WJW. Cell death induced by vaccine adjuvants containing surfactants. Vaccine. 2004b; 22:1524–36. [PubMed: 15063578]

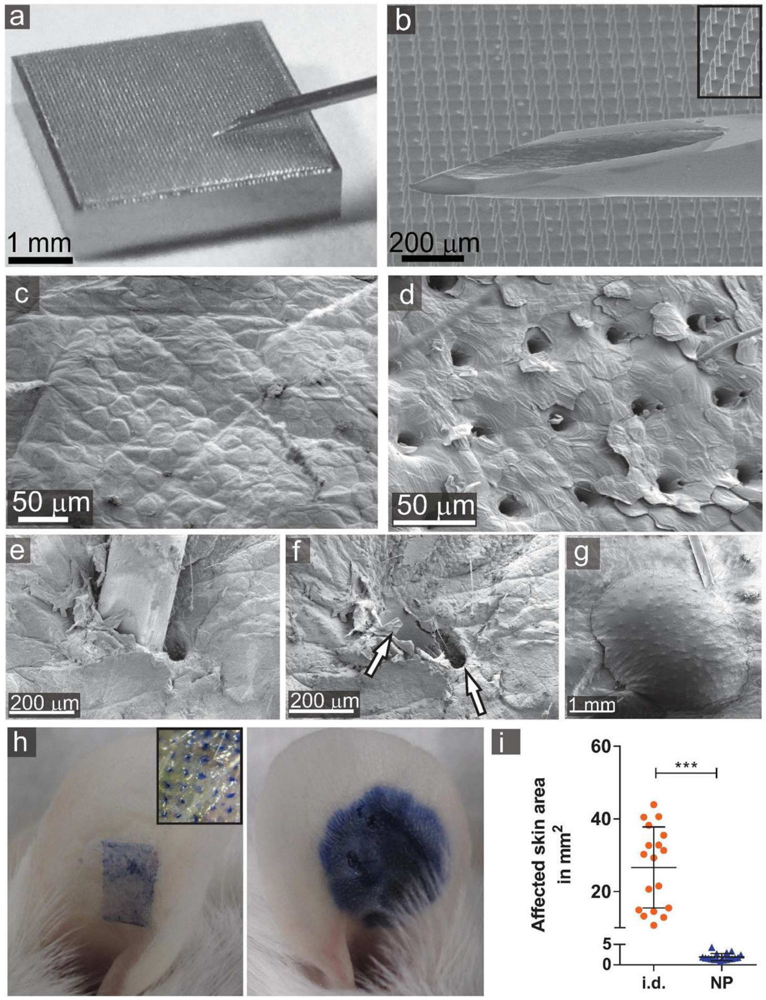

Figure 1. Comparison of the area of affect following Nanopatch application to skin and i.d. injection by hypodermic needle

(a) Size comparison of a NP next to a 31G needle. (b) SEM image of 31G needle tip over NP projections (inset). Cryo-SEM images of murine skin of (c) untreated ear, (d) following NP application, (e) 31G needle i.d. *in situ*, (f) skin after 31G needle removal following delivery of saline, (g) bleb formation following i.d. injection (20 µl saline). Arrows depict the needle insertion site. (h) Coomassie blue administered into mouse ears by either NP (left) or i.d. injection (right). (i) Affected skin surfaces by Coomassie Blue measured in Image J (n=18 applications each). Bar (a, g) = 1 mm, (b, e, f) = 200 µm, (c, d) 50 µm. i.d., intradermal; NP, Nanopatch. Bars represent means ± SD (*** p<0.001).

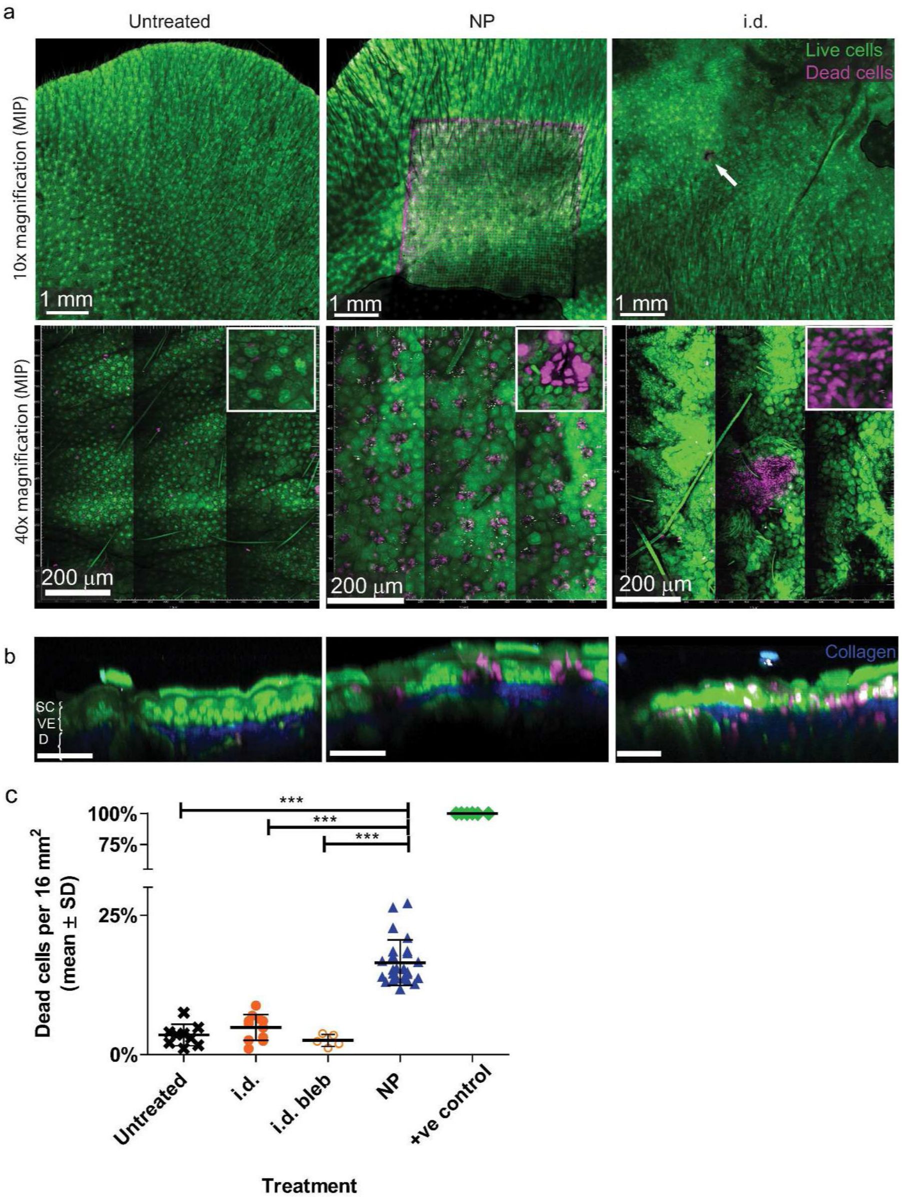

Figure 2. Cell viability in untreated, NP-treated and i.d. saline-injected murine skin

Acridine orange and ethidium bromide were used to differentiate between live (green) and dead (magenta) cells. (a) Multiphoton microscopy images of stained murine; untreated, NP-treated and i.d. injected with high magnification insets. (b) Representative side views of a) with collagen (blue, second harmonic generation). (c) Quantification of cell viability per 16 mm^2; skin incubated in methanol prior to staining as positive cell death control (Skala *et al.*, 2005). Original magnification 10x and 40x. White arrow depicts i.d. injection site. Results are representative of three independent experiments with n=5–8 replicates and up to 3 measurements per replicate. Bar (a, upper panels) = 1 mm, (a, lower panels and b) = 200 µm. MIP, Maximum Intensity Projection; SC, *Stratum corneum*; VE, viable epidermis; D, dermis. Error bars represent means ± SD (*** p<0.0001).

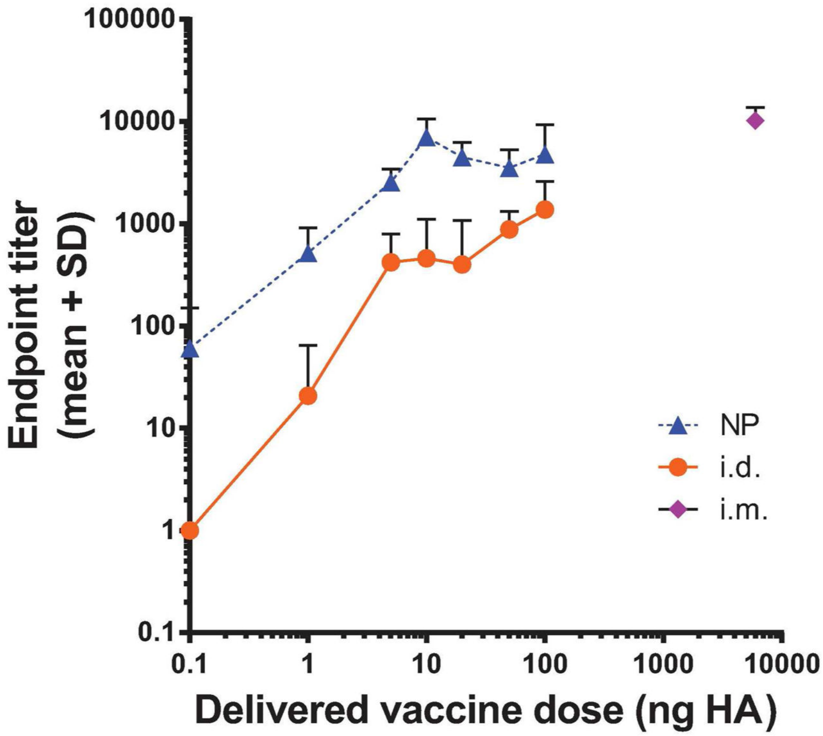

Figure 3. Increased dose-sensitivity to antigen delivered by Nanopatch compared to i.d. injection

Endpoint titers of Fluvax® administered by NP or i.d. injections at various doses (0.1, 1, 5, 10, 20, 50 and 100 ng; i.m. 6000 ng) and analyzed by total IgG ELISA 21 days post immunization. Dose response curve on log scale depicting the dose differences between i.d., NP and i.m.. NP, Nanopatch (▲), i.d., intradermal (●) and i.m., intramuscular (◆). Symbols are means of n=5 and error bars are mean + SD.

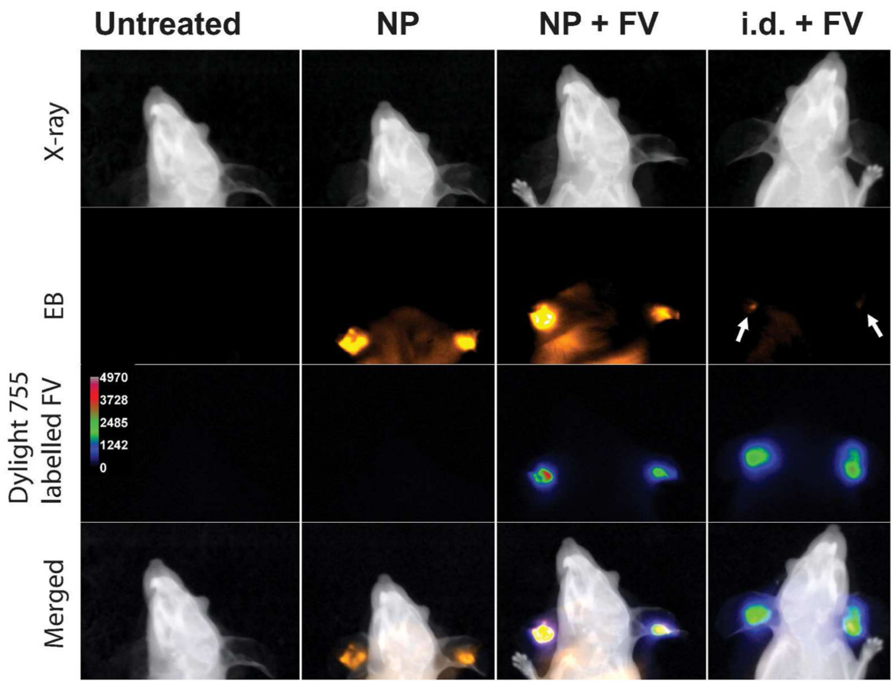

Figure 4. Co-localization of antigen with live and dead cells using Dylight® 755-labelled Fluvax® and viability stain

In vivo imaging of Fluorescent Dylight® 755-labelled Fluvax® (Rainbow colored) administered by NP or i.d. and dead cells (orange) 5 min post administration, detected using a MS FX Pro system overlaid with X-rays (gray scale). Images are representative of n=3 replicates/ group. White arrows depict i.d. injection sites. NP, Nanopatch; i.d., intradermal; EB, ethidium bromide; FV, Fluvax®. Color-coded Dylight® 755 fluorescence represents intensity ranging from high (white-red) to low (blue-black).

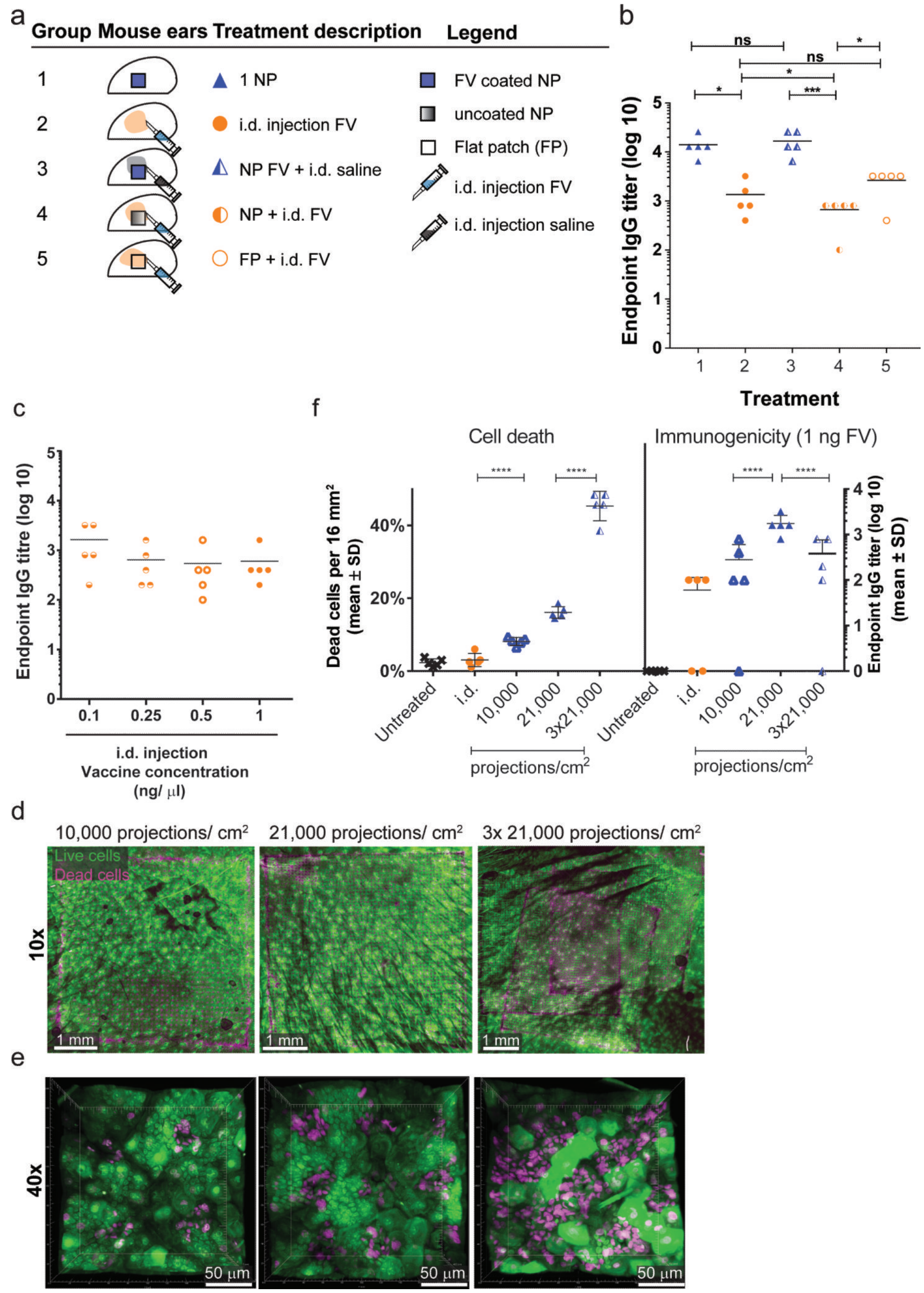

Figure 5. Immune responses to Fluvax® following different levels of induced cell death

(a) Schematic of applied immunizations (b) Fluvax® (10 ng) was delivered by coated NPs, i.d. or a combination thereof (i.d. vaccine delivery followed by NP or FP) into murine ears (control group i.m. 6000 ng). (c) Various Fluvax® concentrations administered i.d. did not affect immunogenicity following i.d. immunization delivering a total of 5 ng Fluvax®. (d) CLSM and (e) MPM imaging of cell death post NP application using various densities (10,000; 21,000; 3x 21,000 projections cm^{-2}). (f) Quantification of cell death linked to Fluvax® immunogenicity (1 ng). All samples were analyzed as previously described. Bar

(d) = 1 mm, (e) = 50 μm. NP, Nanopatch; FP, flat patch; i.d., intradermal; i.m., intramuscular. Depicted are means with n=5 (ns: not significant $p>0.05$,* $p<0.05$, ** $p<0.01$, *** $p<0.001$, **** $p<0.0001$).

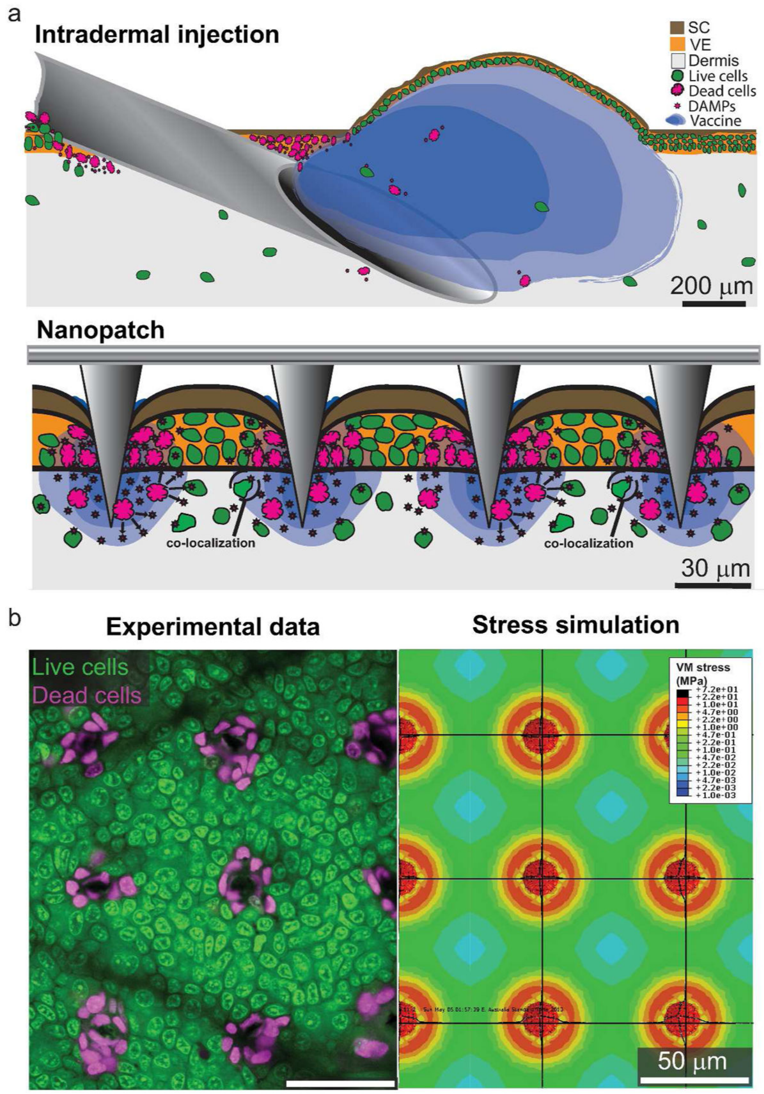

Figure 6. Schematic of i.d. injection and NP delivery alongside live-dead cells, vaccine and proposed DAMPs release and comparison of induced cell death with theoretical stresses in skin

(a) Vaccine (blue) administered either by i.d. injection or dissolving off coated NP projections with cell death (magenta). Vaccine was found predominantly around the i.d. insertion site within the VE and dermis, causing a bleb formation with minimal co-localization of DAMPs (magenta stars) with vaccine and viable cells (green). NP induces highly localized cell death in the VE and minimally in the dermis, with co-localization of DAMPs with antigen and live cells. (b) Comparison of measured cell death with theoretical stresses induced in skin by NP application. Bar (a, upper panel) = 200 μm, (a, lower panel) = 30 μm, (b) = 50 μm. i.d., intradermal; NP, Nanopatch; DAMPs, damage associated molecular patterns; SC, *stratum corneum*; VE, Viable Epidermis.